Implementation and Evaluation of Multi-hop LoRa Networks

Huu Phi Tran and Hoon Oh
Department of Electrical, Electronic and Computer Engineering, University of Ulsan, Ulsan 680-749, South Korea
Email: huuphi.tran88@gmail.com; hoonoh@ulsan.ac.kr

Abstract —A multi-hop approach can extend network coverage, including connectivity to difficult-to-access areas. This paper discusses the implementation and evaluation of the *two-hop real-time LoRa* (Two-hop RT-LoRa) protocol previously proposed to be used for industrial monitoring and control applications. The protocol was implemented on LoRa devices to support a multi-hop LoRa network that consists of one LoRa gateway and 40 end devices. It is shown with various campus deployment scenarios that the protocol improves reliability in data transmission significantly.

Index Terms—Multi-hop LoRa networks, real-time LoRa protocol, implementation, evaluation, reliability

I. Introduction

The LoRa technology has been positively considered for its use in industrial applications due to the high reliability of a wireless link and the simplicity of network topology. Many studies on industry LoRa protocols in academia and industry sectors have been conducted to comply with the need. However, due to its vulnerability to data collision, it is not easy to apply the LoRa technology to industrial applications that not only deal with relatively high traffic, but also require high reliability in data transmission. According to the LoRa specification [1], it is stated that the LoRa channel using even the lowest spreading factor (SF7) can cover the long range of up to km. However, it is not easy to cover even a few hundred miters in the presence of obstructions in industry fields due to signal attenuation if the end devices are installed in *Wireless Unfriendly Zones* (WUZs) such as underground tunnels and enclosed spaces. This study discusses the implementation of the Two-hop RT-LoRa protocol [2], which was proposed recently for industrial use, and evaluates its suitability for industrial applications using various deployment scenarios.

Recently, many studies have been conducted to evaluate the coverage of LoRa and LoRaWAN in various environments. The authors in [3], [4] examined the LoRa network coverage in different experiment scenarios of an indoor environment. According to the results, a LoRa gateway could cover an industrial area of 34,000 m^2 with SF7 and enlarge the coverage by using the higher SFs since the higher SF provides the better receiving sensitivity. In [5], the authors examined the effect of environmental conditions on LoRa communication and showed that the use of the higher SF might not improve reliability in data transmission while consuming much more energy if it comes to an indoor environment that does not ensure line of sight (LOS). Other studies [6]-[10] evaluated the scalability of LoRaWAN by resorting to simulation. It was proven that as the number of nodes increases, data collisions increase sharply because of the random access nature of the Aloha protocol [11].

Some other researches [12]-[14] have focused on designing LoRa protocols for industrial applications. The authors in [12] proposed the *Industrial LoRa* (I-LoRa) protocol that supports both real-time and non-real-time data transmissions. The improved version of I-LoRa, named RT-LoRa [13], was proposed. They use a superframe, as a data collection period, that is divided into a *contention access period* (CAP) for aperiodic data transmission and a *contention-free period* (CFP) for periodic data, during which the Aloha protocol and the slot scheduling approaches are used, respectively. In [14], a real-time LoRa protocol was proposed for *industrial monitoring and control systems* (IMOCSs). The protocol is based on a frame-slot architecture that consists of an *uplink* (UL) and a *downlink* (DL) period, which is further sliced into a number of data transmission slots. The UL data transmissions are scheduled such that the real-time property of data transmissions is guaranteed. Multiple spreading factors are allowed only on different channels to avoid collisions.

The protocols mentioned so far support only a star network topology. The study in [15] presented the needs of multi-hop communication to resolve connectivity on shadow areas and then discussed the concepts and challenges of designing solutions for multi-hop LoRa networks. Even though some multi-hop LoRa protocols [16]-[19] were proposed, they may not be suitable for high traffic industrial applications that require periodic monitoring and high reliability.

To overcome the reliability and coverage problems under high traffic, a two-hop real-time protocol, named Two-hop RT-LoRa, was proposed [2]. This protocol allows nodes to send data based on a slot scheduling for the two-hop topology to prevent the possibility of data collision while it satisfies the real-time requirements of end nodes. In this paper, we studied the applicability of the Two-hop RT-LoRa protocol to real industrial

Manuscript received September 15, 2021; revised March 15, 2022.
Corresponding author email: hoonoh@ulsan.ac.kr.
doi:10.12720/jcm.17.4.273-279

applications. Based on the principle of the protocol, we implemented the functionalities, and then we built the testbed of a LoRa network in two different environments. In the first scenario, twenty end nodes were deployed in one university building and its surrounding area to compare performance between one-hop topology and two-hop topology. Another was deployed across the buildings to examine the suitability of the protocol in the large area that includes a lot of obstructions. According to the experiment, it was proven that the two-hop real-time protocol could not only overcome the reliability problem of one-hop topology, but also cover the large area of 300 x 440 (m^2) with high reliability in data transmission.

II. Two-Hop RT-LoRa Overview

A. Network Topology

A considered LoRa network consists of a *network server* (NS), multiple *gateways* (GWs), and a number of end devices or nodes. GW collects data from participating nodes through LoRa wireless links and forwards the data to NS through a high-speed backhaul network. Nodes are attached to objects or machines in industrial manufacturing environments that are targeted for monitoring and control. A node that can connect to GW directly are said to be *1-hop node*. Meanwhile, some nodes deployed in WUZs may not have a reliable one-hop connection to GW and thus need to establish a two-hop connection to GW via other 1-hop nodes. Such a node is said to be *2-hop node*.

B. Protocol Structure

As shown in Fig. 1, the protocol starts with the *network construction* (NC) period during which two-hop network topology is constructed and then repeats a frame as a *data collection* (DC) cycle to collect data from nodes. Each frame consists of one downlink (DL) period and one uplink (UL) period. The DL period is divided into 2 DL slots: DL#1 for GW to broadcast a DL message and DL#2 for 1-hop nodes to rebroadcast it. The UL period consists of 2^N UL slots, where N is a frame factor ($N \geq 0$). After a number of frames, GW can start the *network maintenance* (NM) period optionally to reflect the changes of network such as node joining or leaving.

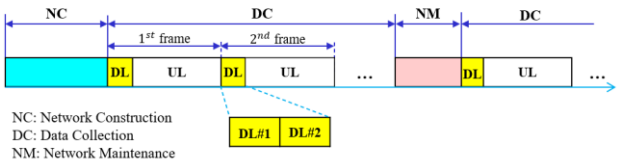

Fig. 1. Protocol operation

C. Task Scheduling for Two-hop LoRa Network

A node is modeled as a *task* as an active entity. For a frame of 2^N slots, a task of node *x*, denoted by τ_x, is characterized by its class *c* as $\tau_x = (c)$ such that its *transmission interval*, $TI(\tau_x)$, is defined as follows:

$$TI(\tau_x) = 2^N / 2^c$$

This indicates that τ_x is required to transmit 2^c packets during one frame period.

Given a set of tasks, the schedule to satisfy the data transmission requirements for each task in the set is generated by a task scheduling algorithm. Task slot scheduling relies on the *logical slot indexing* (LSI) algorithm [14] that assigns a logical slot index to each of 2^N UL slots such that if task τ of class *c* selects 2^c slots sequentially starting with any logical slot index and transmits data in each selected slot, it can meet its time constraints in data transmission. The example of the logical slot indices assigned by the LSI algorithm for the UL period of 16 slots is illustrated in Fig. 2-(a).

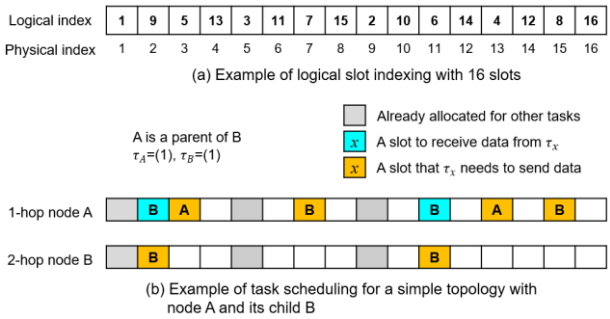

Fig. 2. An example of logical slot indexing and task scheduling

If every node can directly connect to GW, task scheduling becomes easy by using the logical slot indices. However, a 2-hop node requires two slots, one for sending data to its parent and another for the parent to relay the data to GW, while a 1-hop node requires simply one slot to transmit data. Furthermore, if a task takes two slots by using the logical slot indices, the order of the logical slot indices assigned to two slots can be reversed. For example, referring to Fig. 2-(a), consider that a node takes two logical slots 4 and 5 starting with the logical slot number 4 that correspond to physical slot indices 13 and 3, respectively. Then, it has to forward data in physical slot 3 to its parent first, and then the receiving parent has to relay the data in slot 13 to GW. This implies that the physical slot indices corresponding to the logical slot indices have to be sorted in an ascending order to be used for correct data forwarding.

For convenience, let us define the *slot demand* (*SD*) of *h-hop node i*, denoted as $SD^h(i)$, as the number of slots that it requires within one frame. Then, $SD^1(i)$ and $SD^2(i)$ are expressed as follows:

$$SD^1(i) = 2^{class(i)}$$

$$SD^2(i) = 2 * 2^{class(i)}$$

where *class*(*i*) indicates the class of node *i*. Every 1-hop node *i* is required to register its *profile information*, *PF*(*i*), with GW as follows:

$$PF(i) = (i, class(i), PF(i.c_1), PF(i.c_2), ..., PF(i.c_{k_i}))$$

where $i.c_j$ indicates the j^{th} child of node *i*, and k_i is the number of children of node *i*. Then, a *total slot demand* (*TSD*) of a 1-hop node can be calculated as follows:

$$TSD_i = SD^1(i) + \sum_{j \in C(i)} SD^2(j) \quad (1)$$

where *C*(*i*) is the children set of 1-hop node *i*. Then, a server manages the network profile information (*PF*) for the participating nodes as follows:

$$PF = (PF(1), PF(2), ..., PF(n))$$

where *n* is the number of registered 1-hop nodes.

GW distributes *PF* to every participating node by using a DL message. Upon receiving *PF*, a 1-hop node can calculate the *start of the logical slot index* (*startLSI*) by considering the total slot demands of all preceding nodes in *PF*. Then, it can determine its *slot allocation* (*Alloc*) as a set of assigned logical slot indices for itself and its children. Based on its *Alloc* and the given slotted frame, the 1-hop node generates a *local slot schedule* (*LSS*) that includes the *transmitting slots* (*TxSlots*) and *receiving slots* (*RxSlots*) such that *TxSlots* includes the slots to transmit its own data and the slots to relay data received from its children, and *RxSlots* includes the slots to receive data from its children. For detail, readers are referred to the paper [2].

Let us give an example for task scheduling for a simple partial network in which node A has its child node B, both having class 1. Then, *PF*(A) = (A, 1, (B, 1)) and $SD^1(A) = 2$ and $SD^2(B) = 4$. Suppose that the logical slot indices from 1 to 3 have been scheduled for other tasks. Then, since node A has *startLSI* = 4, *Alloc*(A) = (4, 5) and *Alloc*(B) = (6, 7, 8, 9) that correspond to the physical indices (3, 13) and (2, 7, 11, 15) in an ascending order, respectively. The underlined slot numbers indicates the slots in which 1-hop node A relays the data received from 2-hop node B. *TxSlots*(A) = (3, 7, 13, 15) and *RxSlots*(A) = (2, 11). The slot schedule for nodes A and B are illustrated in Fig. 2-(b).

III. Implementation

A. Network Construction

At initialization, GW initiates network construction by broadcasting a *tree construction request* (TCR) message. Then, upon receiving TCR, every node rebroadcasts TCR only once so that the nodes within the coverage of two hops from GW can receive the TCR. In this process, every node determines whether it will become a 1-hop node or a 2-hop node after examining link quality. The link quality is evaluated based on the *received signal strength indicator* (RSSI) and *signal to noise ratio* (SNR) upon receiving TCR. Then, a 2-hop node determines its parent by considering link quality. For the convenience of the experiment, we manually deployed 1-hop nodes and 2-hop nodes by checking signal attenuation between 2-hop nodes and their 1-hop relay nodes and between 1-hop nodes and GW. So, 1-hop nodes, 1-hop relay nodes, and 2-hop nodes were determined as planned beforehand. Every 2-hop node joins its 1-hop parent by sending a *join request* (*JREQ*) message that includes its task profile. Then, every 1-hop node, say node *x*, integrates the profiles of itself and its children into *PF*(*x*) before transmitting it to GW. Then, GW can manage *PF* for all participating nodes.

B. Node Grouping

After the construction of a two-hop network, GW divides 1-hop nodes into multiple groups (G_1, G_2, ..., G_m) for the use of multiple channels on UL data transmission. Then *TSD*(G_i) as the total slot demand of group G_i is given as follows:

$$TSD(G_i) = \sum_{x \in G_i} TSD_x \quad (2)$$

where TSD_x is defined in (1). The grouping is made such that the slot demands of groups are balanced by exploiting the *TSD* of a group in (2). First, the list of all 1-hop nodes are sorted in the descending order of their *TSDs*, and then starting with the first node in the sorted list, each node is included into group *g* such that *TSD*(*g*) is equal to the minimum of all *TSD*(G_i)'s, for *i = 1..m*. The grouping algorithm is given in algorithm 1.

ALGORITHM 1. GROUPING ALGORITHM

Initialization: *NodeList*, G = (G_1, G_2, ..., G_m)
//*NodeList*: A list of all 1-hop nodes
//G: As a set of groups;
sortedList=sort *NodeList* in a *TSD* descending order;
for each *x* such that *x* is the first element in *sortedList* do:
  get group *g* such that *TSD*(*g*) = min{*TSD*(*v*) | *v* ∈ G};
  g = *g* ∪ {*x*};
  sortedList = *sortedList* – {*x*};
endfor

C. Data Collection

Network construction is followed by data collection that is presented as a sequence of frames or data collection cycles. In each frame, GW initiates data collection by broadcasting a DL message in DL#1. Upon receiving the DL message, every 1-hop relay node rebroadcasts it in the following DL#2 so that every node in the network can receive the message. Furthermore, the DL message is utilized for time synchronization and the distribution of scheduling information.

Time synchronization

Suppose that GW broadcasts a DL message at *startDL* given in Fig. 3. Upon receiving the DL message, every 1-hop relay node can calculate its *rebroadcast time*, *startRB*, that corresponds to the start of DL#2, by taking into

account the transmission delay (i.e., ToA: packet time on air) of the DL message as follows:

$$startRB = sysTime() - ToA + DL/2 \quad (3)$$

where *sysTime*() is the local time when the 1-hop node finishes receiving the DL message. Then, 1-hop and 2-hop nodes can calculate their uplink start times *startUL*(*1-hop*) and *startUL*(*2-hop*) as follows:

$$\begin{aligned} startUL(1-hop) &= sysTime() - ToA + DL \\ startUL(2-hop) &= sysTime() - ToA + DL/2 \end{aligned} \quad (4)$$

By using (4), all 1-hop and 2-hop nodes can start their UL periods at the same time.

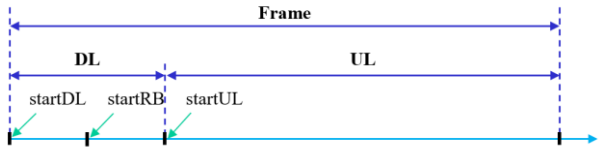

Fig. 3. Time synchronization

Task scheduling

GW distributes the network profile information using the DL message. Since the task grouping is used for the utilization of multiple channels, *PF* can be represented in terms of group profiles as follows:

$$PF = (PF(G_1), PF(G_2), ..., PF(G_m))$$

where $PF(G_i)$ includes the profiles of the nodes that belong to group *i* and is given as follows:

$$PF(G_i) = (PF(1), PF(2), ..., PF(n_i))$$

where n_i is the number of 1-hop nodes in group *i*. Note that every group uses a distinct channel and frame. Upon receiving the DL message, every 1-hop or 2-hop can determine its group to which it belongs and then can generate its own slot schedule easily in the corresponding frame, as illustrated in Fig. 2.

During the UL period, GW receives data from end nodes and saves them for statistics and further processing. If GW didn't receive data from a certain node during a specified number of frames consecutively, it judges that the node is disconnected. If the portion of disconnected nodes is larger than a threshold value, GW initiates the NM period.

IV. Performance Evaluation

A. Experiment I – Setup and Discussion

In this experiment, the effectiveness of a two-hop network is examined using 20 end nodes. The network is deployed over a campus building of 8 floors and its surrounding zones. GW was placed at the right side of the rooftop, and five end-nodes, 15-19, were deployed at the corridors of the 2nd, 3th, and 5th floors inside the building, and 4, 5, 6, and 20 were deployed in the stairways of the building which are open to the outside as shown in Fig. 4-(a) and eleven end-nodes were deployed outside the building as denoted by cyan-colored circles in Fig. 4-(b). In this deployment, only nodes 1, 2, 3, 8, 9, and 10 have a line of sight to GW.

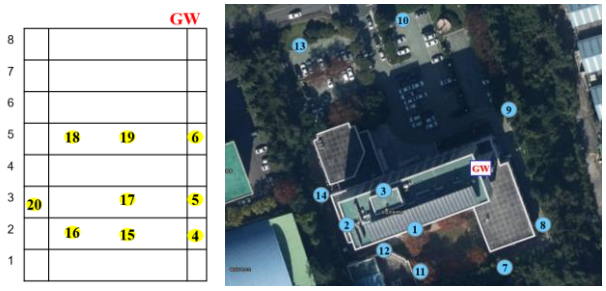

(a) End nodes deployed inside of the building

(b) End nodes deployed outside of the building

Fig. 4. Network deployment in a campus building

The key parameters and values used in this experiment are summarized in Table I.

TABLE I: EXPERIMENT PARAMETERS

Parameter	Value	Parameter	Value
No. nodes	20	UL slot size	100 ms
Payload size	40 bytes	SF, BW	7, 125 kHz
TI	3.6 s	Frame factor	8
DL slot size	200 ms	No. Channels	2

TABLE II: COMPARISON OF PERFORMANCE FOR ONE-HOP AND TWO-HOP TOPOLOGIES

Node	One-hop topology	Two-hop topology	
	PRR	Used relay node	PRR
11	94.5	1	98.6
16	90.0	4	99.3
17	87.0	5	98.7
18	53.2	6	98.1
19	93.7	6	99.4
20	84.6	2	98.7

First, experiment was performed for three hours in the network of 1-hop topology. Most of the end nodes achieved a good *packet reception ratio* (PRR) over 95%; however, nodes 11 and 16-20 given in Table II did not achieve the competent level of PRR. It is worth noting that node 20 showed a low PRR even though it was deployed in the stairway, and node 15 showed high PRR even though it was deployed in the corridor. The reason is that node 20 is located on the opposite side of GW, and node 15 was located by the open lounge in the center of the first floor.

In order to improve the PRR for those unreliable 1-hop nodes, a two-hop topology was built by having each of them use the corresponding relay node as given in Table II. Note that their PRRs were improved greatly to the competent level.

B. Experiment II – Setup and Discussion

A LoRa network of one GW and 40 nodes were deployed to examine the suitability of the protocol in a

large area that includes a lot of obstructions. As shown in Fig. 6, GW was placed in one room on the 6th floor of the building, nodes 6, 19, 20, 31, and 32 were placed around the buildings on the opposite side of GW, nodes 13, 33, and 34 were placed in the spots that are far away from GW, and nodes 39 and 40 were placed inside each of two rooms in two opposite sides along the corridor of the 2nd floor. The pictures for some spots that end devices are placed were given in Fig. 5. The parameter settings are the same as those in Experiment I. Nodes form a two-hop tree topology, as shown in Fig. 6, where the PRR is given next to each node number.

Fig. 5. Some spots of LoRa end devices

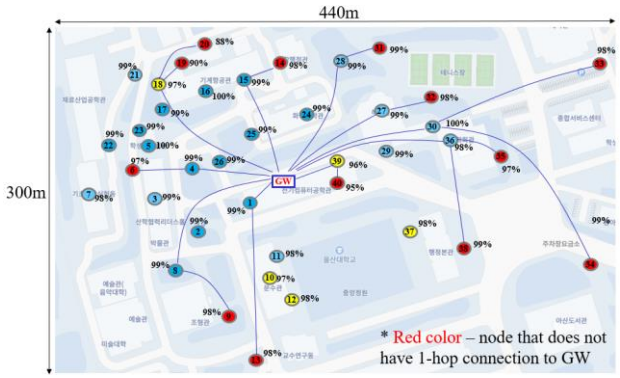

Fig. 6. Network deployment on campus

The red-colored nodes indicate that they cannot connect to GW directly due to signal attenuation by either obstructions or the distance to GW. According to experiment results, it is shown that most of the end nodes achieved a high PRR of above 95% except for end nodes 19 and 20. The reason for the low PRR on nodes 19 and 20 is that the quality of downlink (GW, 18) was not well maintained. In fact, node 18 was disconnected to GW several times, thereby incurring the loss of data from its children. Note that a node does not send data if it fails to receive a DL message at the start of every frame. However, the performance of uplink (18, GW) was well maintained, showing high reliability as PRR of 97%. A similar problem happened to other 1-hop nodes that are yellow-colored. This problem can be explained by the asymmetric link between GW and the end node since they use different LoRa transceivers. According to the SX1301 and SX1276 datasheets, the receiving sensitivity of the LoRa SX1301 transceiver (in GW) was -126.5 dBm while that of the LoRa SX1276 transceiver (in end node) was higher as -123 dBm.

C. *Experiment II – Link Quality*

Maintaining the good quality of links, especially for a link between a relay node and GW, is of great importance for the stable operation of the two-hop protocol. Experiment was performed to examine the downlink quality from GW to 1-hop nodes by having GW broadcast a DL message periodically to nodes in different locations. Every node recorded the average RSSI and SNR and calculated PRR.

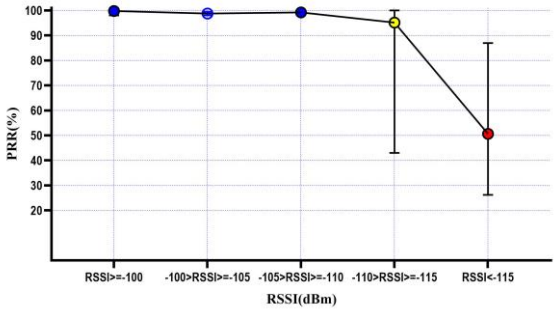

Fig. 7. RSSI vs. PRR

Fig. 7 shows the relationship between the RSSI and PRR values. According to experiment results, nodes with the RSSI value greater than -110 dBm achieved PRR above 98%, and nodes with the RSSI value between -110 dBm and -115 dBm could achieved PRR above 95%. However, nodes with the RSSI value smaller than -115 dBm showed a dramatically decreased PRR down to 51%. Referring to Table III-(a), when the RSSI value of a node falls between -115 dBm and -110 dBm, it can be identified that the link quality of the node is closely related to the SNR value. It is also shown that a node with SNR > -6.0 dB achieves a high PRR greater than 90%. However, when a node has SNR ≤ -6.0 dB, its PRR goes under 71%. Referring to Table III-(b), it is identified that when the RSSI is less than -115 dBm, the SNR values go under -5.7 dB overall, and nodes achieve low PRRs.

TABLE III: EXPERIMENT RESULT FOR RSSI < -110

(a) -110 > RSSI> = -115			(b) RSSI < -115		
RSSI	*SNR*	*PRR*	*RSSI*	*SNR*	*PRR*
-111	-1.8	98.24	-116	-5.7	86.96
-111	-4.8	96.87	-116	-6.9	85.11
-112	-2.4	99.01	-116	-7.4	48.43
-112	-5.6	92.72	-117	-6.1	75.47
-113	-6.0	70.98	-117	-6.4	57.14
-114	-5.3	100	-117	-8.6	35.71
-114	-5.9	93.46	-118	-7.0	50.63
-114	-7.4	43.01	-118	-8.6	26.25
			-118	-8.8	48.08

From the above discussion, it can be concluded that a reliable link with PRR ≥ 95% has RSSI ≥ -115 dBm and SNR ≥ -5.5 dB. This result can be used as a reference to construct a reliable two-hop network.

V. Conclusion

In this paper, we discussed the implementation and experiment of the Two-hop RT-LoRa protocol which was proposed previously. It was shown that the protocol could achieve high reliability in data transmission in indoor and outdoor LoRa network environments. By selecting relay nodes carefully, the protocol could extend network coverage across multiple buildings. Furthermore, it was shown that a two-hop LoRa network could effectively cover a large area of 300x440 (m^2) with high reliability.

Acknowledgement

This work was supported by Institute of Information & communication Technology Planning & Evaluation (IITP) grant funded by the Korea government(MSIT) (2020-0-00869, Development of 5G-based Shipbuilding & Marine Smart Communication Platform and Convergence Service)

Conflict of Interest

The authors declare no conflict of interest

Author Contributions

The authors confirm contribution to the paper as follows: Huu Phi Tran, Hoon Oh conducted the research; Huu Phi Tran implemented the protocol and deployed the experiment scenarios; Huu Phi Tran, Hoon Oh analyzed the data and wrote the paper.

References

[1] Semtech, AN1200.22 LoRa Modulation Bacics, 2015.
[2] H. P. Tran, W. Jung, T. Yoon, D. Yoo, and H. Oh, "A two-hop real-time LoRa protocol for industrial monitoring and control systems," *IEEE Access*, vol. 8, pp. 126239-126252, 2020.
[3] J. Haxhibeqiri, A. Karaagac, F. V. D. Abeele, W. Joseph, I. Moerman, and J. Hoebeke, "LoRa indoor coverage and performance in an industrial environment: Case study," in *Proc. 22nd IEEE International Conference on Emerging Technologies and Factory Automation (ETFA)*, 2017, pp. 1-8.
[4] J. Petäjäjärvi, K. Mikhaylov, M. Hämäläinen, and J. Iinatti, "Evaluation of LoRa LPWAN technology for remote health and wellbeing monitoring," in *Proc. 10th International Symposium on Medical Information and Communication Technology*, 2016, pp. 1-5.
[5] R. Sanchez-Iborra, J. Sanchez-Gomez, J. Ballesta-Viñas, M. D. Cano, and A. F. Skarmeta, "Performance Evaluation of LoRa considering scenario conditions," *Sensors*, vol. 18, no. 3, 2018.
[6] F. V. D. Abeele, J. Haxhibeqiri, I. Moerman, and J. Hoebeke, "Scalability analysis of large-scale LoRaWAN networks in ns-3," *IEEE Internet of Things Journal*, vol. 4, no. 6, pp. 2186-2198, 2017.
[7] M. Bor, U. Roedig, T. Voigt, and J. Alonso, Do LoRa Low-Power Wide-Area Networks Scale? 2016.
[8] J. Haxhibeqiri, F. Van den Abeele, I. Moerman, and J. Hoebeke, "LoRa scalability: A simulation model based on interference measurements," *Sensors*, vol. 17, no. 6, 2017.
[9] A. M. Yousuf, E. M. Rochester, B. Ousat, and M. Ghaderi, "Throughput, coverage and scalability of LoRa LPWAN for internet of things," in *Proc. IEEE/ACM 26th International Symposium on Quality of Service*, 2018, pp. 1-10.
[10] A. Mahmood, E. Sisinni, L. Guntupalli, R. Rondón, S. A. Hassan, and M. Gidlund, "Scalability analysis of a LoRa network under imperfect orthogonality," *IEEE Transactions on Industrial Informatics*, vol. 15, no. 3, pp. 1425-1436, 2019.
[11] N. Abramson, "The aloha system: Another alternative for computer communications," in *Proc. Fall Joint Computer Conference*, 1977, pp. 281-285.
[12] L. Leonardi, F. Battaglia, G. Patti, and L. L. Bello, "Industrial LoRa: A novel medium access strategy for LoRa in industry 4.0 applications," in *Proc. IECON 2018 - 44th Annual Conference of the IEEE Industrial Electronics Society*, 2018, pp. 4141-4146.
[13] L. Leonardi, F. Battaglia, and L. L. Bello, "RT-LoRa: A medium access strategy to support real-time flows over LoRa-Based networks for industrial iot applications," *IEEE Internet of Things Journal*, vol. 6, no. 6, pp. 10812-10823, 2019.
[14] Q. L. Hoang, W. Jung, T. Yoon, D. Yoo, and H. Oh, "A real-time LoRa protocol for industrial monitoring and control systems," *IEEE Access*, vol. 8, pp. 44727-44738, 2020.
[15] H. J. Hwan, D. H. Kim, and J. Kim, "Proposal of seamless communication method in shadow area using LoRaWAN," *Journal of Communications*, 2017.
[16] M. Bor, J. Vidler, and U. Roedig, "LoRa for the internet of things," *EWSN*, pp. 361-366, 2016.
[17] C. Liao, G. Zhu, D. Kuwabara, M. Suzuki, and H. Morikawa, "Multi-Hop LoRa networks enabled by concurrent transmission," *IEEE Access*, vol. 5, pp. 21430-21446, 2017.
[18] H. Lee and K. Ke, "Monitoring of large-area iot sensors using a lora wireless mesh network system: Design and evaluation," *IEEE Transactions on Instrumentation and Measurement*, vol. 67, no. 9, pp. 2177-2187, 2018.
[19] C. Ebi, F. Schaltegger, A. Rüst, and F. Blumensaat, "Synchronous LoRa mesh network to monitor processes in underground infrastructure," *IEEE Access*, vol. 7, pp. 57663-57677, 2019.

Huu Phi Tran received the B.S. degree from the School of Telecommunication Engineering, Xidian University, Xi'an, China, in 2012. He is currently working toward the Ph.D. degree with the Department of Computer Engineering, University of Ulsan, South Korea. His current research interests include embedded systems, wireless sensor networks, and low power wide area networks, etc.

Hoon Oh received the B.S.E.E. degree from the Sung Kyun Kwan University, Seoul, and the M.SC. degree and the Ph.D. degree in computer science from Texas A&M University at College Station, Texas, in 1993 and 1995, respectively. From 1983 to 1989 and 1996 to 2000, he worked as a software engineer and software architect in the Corporate Research Center of Samsung Electronics. He was involved in developing communication protocols for the data services of the CDMA and IMT2000 handset products. Currently, he is a professor of the Department of Computer Engineering and Information Technology and a director of the Vehicle IT Convergence Technology Research Center in University of Ulsan, Korea. He has been serving as a department head of IT convergence department from 2016, University of Ulsan. He received a Best Paper Award from the National Academy of Science, USA in 1995. He published over sixty refereed journals for the last decade and made many technology transfers to the local IT companies through University–industry cooperation program. His research interests lie in embedded systems, mobile ad hoc networks, real-time computing, context-aware computing. He is a member of IEEE, IEICE, and ICASE, and a lifetime member of KICS and KISA.